# Differentiation of SH-SY5Y cells to a neuronal phenotype changes cellular bioenergetics and the response to oxidative stress

**Lonnie Schneider**[1,2,#], **Samantha Giordano**[1,2,#], **Blake R. Zelickson**[1,2], **Michelle Johnson**[1,2], **Gloria Benavides**[1,2], **Xiaosen Ouyang**[2,3], **Naomi Fineberg**[4], **Victor M. Darley-Usmar**[1,2], and **Jianhua Zhang**[1,2,3,*]

[1]Center for Free Radical Biology, University of Alabama at Birmingham

[2]Department of Pathology, University of Alabama at Birmingham

[3]Department of Veterans Affairs, Birmingham VA Medical Center

[4]Department of Biostatistics, UAB School of Public Health

## Abstract

Cell differentiation is associated with changes in metabolism and function. Understanding these changes during differentiation is important in the context of stem cell research, cancer, and neurodegenerative diseases. An early event in neurodegenerative diseases is the alteration of mitochondrial function and increased oxidative stress. Studies using both undifferentiated and differentiated SH-SY5Y neuroblastoma cells have shown distinct responses to cellular stressors, however the mechanisms remain unclear. We hypothesized that since the regulation of glycolysis and oxidative phosphorylation are modulated during cellular differentiation, this would change bioenergetic function and the response to oxidative stress. To test this, we used retinoic acid (RA) to induce differentiation of SH-SY5Y cells and assessed changes in cellular bioenergetics using extracellular flux analysis. After exposure to RA, the SH-SY5Y cells had an increased mitochondrial membrane potential, without changing mitochondrial number. Differentiated cells exhibited greater stimulation of mitochondrial respiration with uncoupling and an increased bioenergetic reserve capacity. The increased reserve capacity in the differentiated cells was suppressed by the inhibitor of glycolysis, 2-deoxy-D-glucose (2-DG). Furthermore, we found that differentiated cells were substantially more resistant to cytotoxicity and mitochondrial dysfunction induced by reactive lipid species 4-hydroxynonenal (HNE) or the reactive oxygen species generator 2,3-dimethoxy-1,4-naphthoquinone (DMNQ). We then analyzed the levels of selected mitochondrial proteins and found an increase in complex IV subunits which we propose contributes to the increase in reserve capacity in the differentiated cells. Furthermore, we found an increase in MnSOD that could, at least in part, account for the increased resistance to oxidative stress. Our findings suggest that profound changes in mitochondrial metabolism and antioxidant defenses occur upon differentiation of neuroblastoma cells to a neuron-like phenotype.

[*]**Corresponding author:** Jianhua Zhang, Ph.D., Department of Pathology, University of Alabama at Birmingham, BMRII-534, 901 19th Street South, Birmingham, AL 35294-0017, USA, Phone: 205-996-5153; Fax: 205-934-7447; zhanja@uab.edu.
[#]Co-first Author

The authors have no conflict of interest.

## Introduction

Mitochondrial dysfunction and oxidative stress are early characteristics and key contributing factors to neurodegeneration in diseases, including Parkinson's disease (1). Post-mitotic neurons are highly dependent on mitochondria to meet their bioenergetic demands, in contrast to rapidly dividing cells or tumor cells that largely depend upon glycolysis as a primary energy source (2). Neuronal cells maintain a bioenergetic capacity sufficient to meet physiological energy demands with a reserve or spare capacity which can be utilized by the cells under stress (2). For example, during signal transmission across synapses, neurons have high energy demands that maintain and allow rapid recovery from depolarization (3). Bioenergetic reserve capacity is utilized when excessive glutamatergic stimulation causes a cellular $Ca^{2+}$ overload and increased energy demand in the cell (4). The recruitment of the bioenergetic reserve capacity under these conditions is essential to prevent cell death (4). Additionally, post-mitotic neurons cannot divide to remove or dilute out damaged components and do not have high levels of antioxidants when compared to other cells, such as the glia making their bioenergetic capacity a potentially important factor in protecting against oxidative stress (5).

In a recent series of studies, we and others have proposed that the reserve or spare bioenergetic capacity is critical to resist the toxicity associated with increased oxidative stress (6). In the case of neurodegenerative diseases, such as Parkinson's, in which mitochondrial respiratory chain proteins are damaged (7), reserve capacity is likely to be compromised rendering the cells more susceptible to oxidative insults. It has been suggested by the Warburg hypothesis that rapidly dividing undifferentiated cells have a greater dependence on glycolysis for metabolic intermediates needed for cell division (8–10). This also results in a down regulation of mitochondrial function which suggests that the mitochondria maybe functioning at near maximal rates resulting in loss of bioenergetic reserve capacity. This paradigm also suggests that as cells differentiate, the metabolic requirements change, resulting in a greater requirement for mitochondrial ATP production. In the present study, we have used the well-established cell line SH-SY5Y because it can be maintained in an undifferentiated state, and can be stimulated to differentiate into a neuron-like phenotype in cell culture (11–18). SH-SY5Y human neuroblastoma cells are derived from a thrice cloned cell line SK-N-SH originally from a neuroblastoma patient (19). SH-SY5Y cells contain many characteristics of dopaminergic neurons (11), and have therefore been used extensively to study neuron-like behavior in response to neurotoxins in the context of Parkinson's disease (11).

Neurodegenerative diseases are frequently associated with increased oxidative stress, including increased production of lipid peroxidation products (20;21). An important secondary lipid peroxidation product that is present in Parkinson's disease brain is the aldehyde 4-hydroxy-2-nonenal (HNE). HNE is electrophilic, which allows it to react with nucleophilic protein residues, thus modulating their functions (22–28). Furthermore, accumulation of HNE can damage key proteins in the mitochondrial respiratory chain (29;30), inhibit NADH-linked respiration (31;32), and deplete cardiolipin (33). In addition the ability of the mitochondria to resist the toxic effects of reactive lipid species has not been investigated in this neuronal cell model and was tested in the present study. Using both undifferentiated and differentiated SH-SY5Y cells as a model system, we characterized the mitochondria and the bioenergetics of these cells under basal conditions and in response to oxidative stress induced by exposure to the oxidized lipid HNE and the generator of intracellular reactive oxygen species (ROS), 2,3-dimethoxy-1,4-napthoquinone (DMNQ) (34). This is particularly relevant to Parkinson's disease because hydrogen peroxide is produced by dopamine metabolism and is thought to be a major contributor to the early dopaminergic cell death (35). In the present study we compared susceptibility to DMNQ and

HNE in differentiated and undifferentiated cells and propose that mitochondrial function plays a key role in the differential response to oxidative stress in neuronal cells.

## Materials and Methods

### Materials

HNE was obtained from Calbiochem. DMNQ (2,3-dimethoxy-1,4-napthoquinone) was obtained from Alexis Biochemicals. All materials for the Extracellular Flux assays were from Seahorse Biosciences. Carbonyl cyanide *p*-[trifluoromethoxy]-phenyl-hydrazone (FCCP), oligomycin, and antimycin A were from Sigma. MitoTracker Red was purchased from Molecular Probes. JC-1 was purchased from Invitrogen.

### Cell cultures

We cultured and used early passage P11-17 human neuroblastoma SH-SY5Y cells grown in DMEM supplemented with 10% fetal bovine serum, 2 mM glutamine, and penicillin/ streptomycin. Differentiation was induced by 10 µM all-trans retinoic acid on day 1 after plating and continued for 5 days. Medium was replaced with fresh medium containing retinoic acid every 48 hours in 1% DMEM supplemented with 1% fetal bovine serum, 2 mM glutamine and penicillin/streptomycin.

### Immunocytochemistry

Cells were grown in 24 well plates in which a glass coverslip was added to the well prior to plating. Cells were fixed with 4% paraformaldehyde for 1 h at room temperature, permeabilized by 0.1% Triton X-100, incubated in 5% BSA blocking buffer for 1 h, followed by primary antibodies and then Cy3 or FITC conjugated secondary antibodies, and countered stained with Hoechst. Glass cover plates were taken out and mounted to glass slides. Staining was visualized on a Leica TCS SP5 confocal microscope. MitoTracker images were taken for live cells grown on chamber slides using the same Leica TCS SP5 confocal microscope.

### Measurement of mitochondrial membrane potential by JC-1 staining

Cells were washed with phenol red and serum free DMEM media, then incubated the cells with 5 µg/ml of JC-1 in phenol red and serum free DMEM for 45 min. Cells were then washed 3 times with serum free DMEM. The last wash was without (Control) or with 10 µM FCCP (FCCP). The cells were incubated in media or media + FCCP for 10 min and then were imaged on a Perkin Elmer Life Sciences Wallace 1420 multilabel plate reader. Green was imaged with 485 nm excitation and 530nm emission and red was imaged with 530 nm excitation and 590 nm emission. The ratio of red/green fluorescence (aggregated/non-aggregated JC-1) was calculated.

### Assessment of cell viability

We measured cell viability using a MTT [3-(4,5-dimethylthiazol-2-yl)-2,5-diphenyl-2*H*-tetrazolium bromide] assay as described previously (29;36), and confirmed by a Calcein AM assay and cell counting by trypan blue exclusion. For MTT assay, we seeded SH-SY5Y cells in the XF24 culture plates at 80,000 cells/well. Sixteen hours after HNE or DMNQ treatment, the cells were incubated with media containing 0.4 mg/ml thiazoyl blue tetrazolium in a 37°C incubator for 2 h. Then we removed the media, solubilized the resulting formazan crystals in 250 µl DMSO, and read the absorbance at 550 nm.

### Citrate synthase assay

Citrate synthase activity is based on the reaction of Ellman's reagent, DTNB (5,5'-Dithio-bis(2-nitrobenzoic acid) with the thiol group of free CoA producing TNB (5-thio-2-nitrobenzoic acid) measured at 412 nm. Whole cell lysates were incubated with 100 mM Tris/0.1% (v/v) Triton X-100, pH 8.0 containing 0.2 mM DTNB, 0.1 mM Acetyl CoA. Reactions were initiated by the addition of oxaloacetate (0.2 mM). Rates are reported as nmol TNB formed/min/mg protein.

### Quantification of mtDNA

DNA was extracted from SH-SY5Y cells at the indicated days of differentiation. Quantitative real-time PCR was performed by using a LightCycler-DNA Master SYBR Green I kit (Roche) as described previously (37). The primer sequences used for mtDNA were: mtF (5′-CACCCAAGAACAGGGTTTGT-3′) and mtR (5′-TGGCCATGGGTATGTTGTTAA-3′). The primer sequences for the nuclear DNA (nDNA) were 18SF (5′-TAGAGGGACAAGTGGCGTTC-3′) and 18SR (5′-CGCTGAGCCAGTCAGTGT-3′). Cycling conditions were as follows: 95°C for 150 s, followed by 40 cycles at 95°C for 10 s, 58°C for 15 s, and 72°C for 20 s.

### Measurement of mitochondrial function

To measure mitochondrial function in differentiated and undifferentiated SH-SY5Y cells, a Seahorse Bioscience XF24 Extracellular Flux Analyzer was used. The XF24 creates a transient, 7 µl chamber in specialized microplates that allows for the determination of oxygen and proton concentrations in real time (38;39). To allow comparison between different experiments, data are expressed as the rate of oxygen consumption in pmol/min or the rate of extracellular acidification in mpH/min, normalized to cell protein in individual wells determined by the DC protein assay (BioRad). In some experiments the data were expressed as a percentage of the basal $O_2$ consumption rate (OCR) or extracellular acidification rate (ECAR). The optimal seeding density of the cells needed to obtain a measurable $O_2$ consumption and extracellular acidification rates (OCR and ECAR respectively) was established, and both ECAR and OCR show a proportional response with cell number (data not shown). For subsequent experiments, a seeding density of 80,000 cells per well was selected to allow both potential increases and inhibition of OCR and ECAR to be assessed. The undifferentiated and differentiated cells grew at different rates which could confound the interpretation of the data. To address this issue we undertook a comprehensive analysis of the relationship between basal and maximal OCR and ECAR for the cells at different cell densities so removing this factor as an uncontrolled variable by using protein levels in individual wells as an index of cell number (Supplemental Figure 1 A–D) (Dranka et al 2011, FRBM in press) (3). We have noted that high levels of FCCP inhibit mitochondrial respiration presumably due to the loss of the ability to accumulate respiratory substrates. Accordingly, oligomycin, FCCP, and antimycin A concentrations to elicit maximal effects were optimized prior to assessment of bioenergetic function and found to be 1 µM, 1 µM and 10 µM respectively.

### Western blot analysis

Protein extracts were separated by SDS-PAGE and probed with respective antibodies. Antibodies used: MAP2 (Sigma), Complex I-subunit 39 kDa (Invitrogen), Complex I ND1 (Abcam), Complex III-FeS (Invitrogen), Complex IV-subunit II (Invitrogen), Complex IV-subunit IV-isoform 1 (Abcam), Complex IV-subunit IV-isoform 2 (Protein Tech), VDAC (MitoSciences), MnSOD (Assay Design), and Bcl-2 (Santa Cruz). Ponceau S staining was used to demonstrate equal loading. Relative levels of proteins were quantified by densitometry using AlphaEase software from Cell Biosciences (Santa Clara, California).

### Statistical analysis

Data are reported as mean ± SEM. Comparisons between two groups were performed with unpaired Student's *t*-tests. Comparisons among multiple groups or between two groups at multiple time-points were performed by either one-way or two-way analysis of variance, as appropriate. A *p* value of less than 0.05 was considered statistically significant. For data presented in Supplemental Figure 1, the data were collected under two treatment conditions (control and retinoic acid) over three independent experiments. Within each experiment, 4–5 wells were studied for each treatment condition. Protein levels and basal and maximal OCR were measured for each well. Repeated measures analysis of covariance (RM ANOCVA) was performed to analyze significance between treatment groups and between experiments. Experiment and treatment were considered grouping factors and protein levels were a covariate. The basal and maximal OCR measurements in each well were considered the repeated measures.

## Results

### Differentiation of SH-SY5Y cells and mitochondrial characterization

Exposure of SH-SY5Y cells to retinoic acid (RA) results in differentiation to a more characteristically neuronal morphology (11). Prior to determining whether differentiation changes cellular bioenergetics, we first performed a series of studies characterizing mitochondria in both undifferentiated and differentiated SH-SY5Y cells. As shown in Figure 1A, cells at Day 0 exhibit compact morphology which changes over days 3–5 on exposure to RA with formation of axons and dendrite-like projections and shrinkage of the cytoplasm. In previous studies (11–18), and as shown in Figure 1A, an important feature of differentiation is the extension of neurites. In addition differentiation results in increased expression of the neuronal marker, microtubule associated protein 2 (MAP2). The fluorescence intensity of MAP2 was found to have increased by 50% after 5 days exposure to RA (Figure 1B,C). Next cells were stained with MitoTracker Red under the same conditions as Figure 1 (Figure 2A). As the cells adopt a more differentiated phenotype, the mitochondrial network is now distributed throughout the cell into the neurites. Mitochondrial membrane potential was assessed by JC-1 and found to increase approximately 60% at Day 5 after RA treatment (Figure 2B) and, as expected, the uncoupler FCCP decreased mitochondrial membrane potential in both undifferentiated and differentiated cells.

Cell lysates were collected after 5 days of RA, to assess potential changes in mitochondrial mass or number. The mitochondrial matrix enzyme, citrate synthase is frequently used as an index of mitochondrial number and was not changed by RA treatment (Figure 2C) and this overall conclusion was confirmed by measurement of mitochondrial DNA copy number normalized to nuclear DNA copy number, which also did not change (Figure 2D).

### Differentiation of SH-SY5Y cells increases their mitochondrial bioenergetic reserve capacity

To determine whether treatment with RA impacts cellular bioenergetics we assessed mitochondrial function in both undifferentiated and differentiated SH-SY5Y cells. Extracellular flux analysis allows determination of $O_2$ consumption and extracellular acidification in adherent cells (39;40) (Dranka et al 2011, FRBM in press). The basal $O_2$ consumption rates (OCR) in both undifferentiated and differentiated cells (RA treatment for 5 days) are not significantly different (Figure 3A,B). This value is also comparable to the published rate of 8.8 pmol of $O_2$/min/µg protein measured by polarography for these cells (41;42). We next defined mitochondrial function in differentiated and undifferentiated SH-SY5Y cells by sequentially adding pharmacological inhibitors of the respiratory chain (Figure 3A,B) (3). After measurement of basal OCR, oligomycin (1 µg/ml) was injected into

all samples to inhibit the ATP synthase (Complex V). In both forms of the SH-SY5Y cells a substantial decrease in OCR occurred to approximately the same extent indicating that the mitochondrial oxygen consumption used for ATP synthesis is not changed during cellular differentiation.

The remaining OCR, after oligomycin treatment, can be ascribed to both proton leak across the mitochondrial membrane and utilization of the mitochondrial membrane potential for ion or substrate transport (43). It is important to note that oligomycin induces a state 4-like respiratory condition which causes an increase in the mitochondrial membrane potential ($\Delta\Psi_m$) (44) and a higher proton leak through the mitochondrial membrane (45;46). Thus the value determined here for proton leak will be overestimated by approximately 10–15% (6).

Next, to determine the maximal OCR that the cells can sustain, the proton ionophore (uncoupler) FCCP (1 µM) was injected. We have noted that high levels of FCCP inhibit mitochondrial respiration, presumably due to the loss of the ability to accumulate respiratory substrates, therefore the FCCP concentration was titrated in both differentiated and undifferentiated cells to determine the concentration that gave the maximum response (1 µM). FCCP addition resulted in stimulation of OCR which is due to the increase in permeability of the mitochondrial inner membrane to protons, resulting in an OCR unconstrained by the mitochondrial membrane potential. The OCR after addition of FCCP is then an estimate of the potential maximal respiratory capacity. Interestingly, the maximal respiratory capacity in the undifferentiated cells was essentially identical to the basal respiratory OCR. The potential reserve capacity for bioenergetic function in the cells is calculated by subtracting the basal OCR from the maximal OCR. We therefore conclude that the undifferentiated cells have no significant bioenergetic reserve capacity (Figure 3B). In contrast, the maximal respiratory capacity was stimulated 25–40% in the differentiated cells, and the reserve capacity is substantially increased in the differentiated cells to essentially the maximal level at 5 days after exposure to retinoic acid (Figure 3C, Supplementary Figure 1). Lastly, antimycin A (10 µM) was injected to inhibit electron flux through Complex III which causes a dramatic suppression of the OCR. The remaining OCR is attributable to $O_2$ consumption due to the formation of mitochondrial ROS and non-mitochondrial $O_2$ consumption and is unchanged by differentiation of the SH-SY5Y cells.

RA treatment for 24 hr did not induce reserve capacity (Figure 3C) suggesting that changes in bioenergetic function are not an immediate response to the addition of RA. Reducing serum alone for 24 hr to 1% FBS also did not change reserve capacity (data not shown), suggesting that the increase of reserve capacity is not simply due to decreased cell proliferation or ATP demand. Using these data we can estimate the metabolic status of the mitochondria in a cellular setting and compare it to the states of respiration previously defined for isolated mitochondria (6). In this analysis, we assume that state 4 respiration is equivalent to the OCR after addition of oligomycin since the cells will be unable to use the proton gradient to generate ATP. Similarly, we assume that state 3 respiration is equivalent to the OCR after the addition of FCCP. Using these parameters we calculated the State$_{apparent}$ for both undifferentiated and differentiated SH-SY5Y cells. The State$_{apparent}$ for undifferentiated cells is (3.04) suggesting that proliferating undifferentiated cells are functioning at or close to their maximal bioenergetic capacity (State 3). After exposure to RA for 5 days, the State$_{apparent}$ for SH-SY5Y cells moves closer to State 4 (3.40), indicating that the cells respire at an intermediate respiratory state. This implies that the function and control of the electron transport chain has changed as a result of differentiation, potentially affording the differentiated cells a higher bioenergetic capacity to utilize under increased work demand or stress.

Under the identical conditions shown in Figure 3A, the ECAR was also determined. Several studies have demonstrated conclusively that this measurement reflects glycolytic activity in the cells (47). Figure 3D shows the ECAR for the undifferentiated and differentiated cells before (basal) and after the injection of oligomycin (maximal) (see also supplementary Figure 1). Under basal conditions, ECAR is decreased in differentiated cells compared to undifferentiated cells, but the increase in the presence of oligomycin is higher in the differentiated cells (2 fold compared to $1.4 \times$ fold in undifferentiated cells). These data are consistent with a higher glycolytic activity in undifferentiated cells.

To test the contribution of glycolysis to the increased reserve capacity in differentiated cells, we used 2-deoxy-D-glucose (2-DG) as an inhibitor. Basal OCR was decreased by 2-DG in differentiated cells and reduced maximum OCR in both undifferentiated (Figure 4A) and differentiated cells (Figure 4B). Reserve capacity is significantly decreased by 2-DG in differentiated cells, suggesting a significant contribution of glycolytic activity to provide substrates for maximal bioenergetic capacity in these cells (Figure 4B). In the presence of 2-DG, ECAR is no longer increased by oligomycin in both undifferentiated and differentiated cells (data not shown).

## Differentiation of SH-SY5Y cells confers resistance to oxidative stress-induced cell death and alterations of mitochondrial function

We measured the survival of undifferentiated and differentiated cells in response to HNE, a reactive lipids species, and DMNQ, an intracellular generator of ROS. We found that differentiated SH-SY5Y cells are more resistant than undifferentiated cells to HNE (Figure 5A) and DMNQ (Figure 5B) -induced cell death. We further hypothesized that mitochondrial dysfunction in response to these oxidative stressors is an early event before cell death occurs. To determine the impact of HNE on the parameters of mitochondrial function, the basal OCR in SH-SY5Y cells was determined, followed by OCR measurement after the addition of HNE.

As shown in Figure 6A, both basal and maximal OCR in undifferentiated cells is dose-dependently reduced by HNE. At 20 µM, there is no remaining maximum OCR, indicating mitochondrial function is eliminated by HNE at this concentration. In differentiated cells, HNE also reduced both the basal and maximal OCR but to a lesser extent than in undifferentiated cells (Figure 6B). The comparison of basal OCR 25 min after HNE exposure was plotted in Figure 7A and shows a greater HNE-dependent inhibition for the undifferentiated cells suggesting they are initially more susceptible to stress. The values of maximal OCR, assessed after addition of FCCP, in undifferentiated and differentiated cells are shown in Figure 7B. The reserve capacity was calculated by subtracting the basal OCR at the time point immediately prior to the addition of oligomycin from maximal OCR. The reserve capacity values in undifferentiated and differentiated cells are plotted in Figure 7C and show an HNE-dependent decrease in reserve capacity in differentiated cells. Similarly, we examined cellular bioenergetics in both undifferentiated and differentiated SH-SY5Y cells after 4 h treatment with DMNQ. DMNQ dose-dependently reduced basal and maximal OCR in undifferentiated cells but had no effect on basal and maximal OCR in differentiated cells (Figure 8,9). DMNQ only decreased the reserve capacity in differentiated cells at the highest concentration (Figure 9).

To determine the molecular mechanisms responsible for the increased reserve capacity and resistance to oxidative stress, we examined the levels of mitochondrial proteins in cell lysates in undifferentiated and differentiated SH-SY5Y cells. Western blot analyses showed no change in complex I subunit 39kDa, complex I ND1, complex III Fe-S, complex Vβ, outer membrane protein VDAC, or Bcl-2. Interestingly, we found an increase in the matrix

protein MnSOD (approximately 4 fold) and an increase in complex IV subunit II, and subunit IV-isoforms I and 2 (Figure 10).

## Discussion

SH-SY5Y cells are frequently used to study neuron-like behavior in response to neurotoxins in the context of Parkinson's disease (11), because they possess many characteristics of dopaminergic neurons (11–18). The SH-SY5Y cells can be prepared in both the undifferentiated and differentiated forms, and both types have been widely used in Parkinson's disease research, despite the ongoing debate as to which cell is the most appropriate model. On one hand, it has been noted that differentiation by retinoic acid confers resistance to oxidative stress inducing compounds such as 6-hydroxydopamine whereas neuronal cells are generally thought to be more susceptible (15). The authors conclude that differentiated cells are not the best model to study toxicity mediated by agents such as 6-hydroxydopamine. On the other hand, undifferentiated cells have biochemical and morphological characteristics of early sympathetic neurons with few mature neuronal markers (11;48). This has raised the question whether undifferentiated cells are suitable to study the effects of neurotoxins relevant to adult neurodegenerative diseases since these diseases primarily affect mature fully differentiated neurons. Supporting this notion, a separate study has reported that RA differentiated cells are more sensitive to 6-hydroxydopamine (13). How differentiation changes cellular bioenergetics is therefore an important question in understanding neurodegeneration. Recently, Birket et al. have shown that the oxidative phosphorylation in human embryonic stem cells (hESCs) decreases as the cells differentiate into hESC-derived neural stem cells (NSCs). During differentiation there is a decrease in overall ATP turnover, macromolecule biosynthesis and protein secretion (49). The controversial findings in SH-SY5Y cells and the new studies on embryonic stem cell development prompted us to determine the response of cellular bioenergetics to differentiation in SH-SY5Y cells. Specifically, we reasoned that measuring bioenergetic reserve capacity may provide insight into how oxidative stress differentially impacts cellular bioenergetics and be useful in determining the applicability of differentiated SH-SY5Y cells to the study of neurodegenerative diseases.

In this study, we found that RA-induced differentiation alters mitochondrial function in SH-SY5Y cells. Specifically, we found RA increases mitochondrial membrane potential, levels of cytochrome c oxidase and MnSOD and bioenergetic reserve capacity. The lack of major changes in citrate synthase activity and in complex I subunit 39 kDa, complex I ND1, complex III Fe-S, complex Vβ, VDAC, or Bcl-2 suggests that the changes in mitochondrial function are relatively specific, although a complete proteomics analysis is required to address this point. Differentiation increases the cells' ability to combat stress and confers additional protection from HNE- and DMNQ-induced mitochondrial dysfunction and cell death. Interestingly, during these changes in mitochondrial function, there are no increases in total mitochondrial DNA copy number as shown in Figure 2D, or the activity of the matrix enzyme citrate synthase as shown in Figure 2C.

From the mitochondrial function studies (Figure 3), the fact that the State$_{apparent}$ is closer to State 4 and the mitochondrial membrane potential is higher suggests that the mitochondria are metabolically less active in the differentiated cells. This could occur for a number of reasons, including a decreased ATP demand in the differentiated cells or an increased capacity of the respiratory chain. The undifferentiated cells are rapidly dividing and could therefore have a higher ATP demand. However, the ATP linked OCR is identical in both differentiated and undifferentiated cells (Figure 3B), which does not support an increased ATP demand. More likely the increased reserve capacity reflects the increased levels of cytochrome c oxidase (Figure 10). In addition, it is important to recognize that differentiated

cells maybe utilizing glycolysis and oxidative phosphorylation to serve different purposes than the dividing undifferentiated cells.

In this regard, we found that undifferentiated SH-SY5Y cells have higher intrinsic basal ECAR (approximately 80% of maximum) than differentiated cells (50% of maximum). This suggests that the undifferentiated cells are more reliant on glycolysis to sustain ATP demand. Indeed it is known that cancer cell lines have greater requirement for intermediates of the TCA cycle for cell division resulting in a lower control of respiration in these cells by ADP (5;8–10;50). In support of this possibility the basal OCR in the undifferentiated cells was more sensitive to the inhibitor of glycolysis, 2-DG, than differentiated cells (Figure 4).

Reserve capacity is a parameter which has been proposed to be necessary for cells to survive stressors such as $Ca^{2+}$ overload, reactive oxygen and nitrogen species (ROS/RNS) and oxidized lipids (2;4;6;29;51–53). Prior studies with characterization of mitochondrial function in primary neurons have revealed that mature neurons indeed exhibit reserve capacity (38). Due to the post-mitotic nature of this cell, it is important to maintain this reserve capacity to survive stress, whereas proliferating cells use much bioenergetic function to divide, as discussed above. It has been shown that reserve capacity is important in Parkinson's disease, a neurodegenerative disease with a strong oxidative stress component (54). Cybrid NT2 cells with mitochondria from Parkinson's disease patient platelets exhibited similar basal OCR as parent NT2 cells, whereas in the cybrid cell, reserve capacity is significantly reduced (54).

The differentiated cells were more resistant to the stress of 4-HNE or DMNQ (Figure 6–9). The redox cycling agent DMNQ enters cells and generates both superoxide and hydrogen peroxide at a concentration-dependent rate, similar to reactive oxygen species (ROS) generated by endogenous enzymes, such as NADPH oxidase. Since we found a substantial increase in MnSOD, this clearly can contribute to the protection against DMNQ. Indeed, MnSOD has previously been shown to be induced by retinoic acid in SK-N-SH cells and is postulated to play an important role in differentiation by decreasing oxidative stress (55). However, it is not obvious why the toxicity of 4-HNE should be decreased by MnSOD unless the reactive lipid species promotes mitochondrial ROS formation as we have previously shown in endothelial cells (56). Another possibility is that the increased reserve capacity may provide a greater energetic reserve for the repair of protein and lipid damage mediated by ROS. Our prior studies have shown that changes of complex IV may make electron transfer chain more efficient (57), and thus may provide a mechanism for increased reserve capacity. High reserve capacity has been shown to be important in defense against oxidative stress in vascular cells (6). Further studies will determine whether both MnSOD and complex IV changes are required for reserve capacity and resistance to oxidative stress. Our findings suggest that exploration of approaches that target the mitochondrion, especially ones which increase mitochondrial reserve capacity and control ROS, may provide novel neuroprotective mechanisms for cellular preservation and protection against oxidative stress.

Highlights
> SH-SY5Y cells adopts a more oxidative phenotype on differentiation.> Differentiated SH-SY5Y cells haves increased cytochrome c oxidase and MnSOD. >Bioenergetic reserve capacity is increased in the differentiated SH-SY5Y cells. >Differentiated SH-SY5Y cells are more resistant to oxidative stress.

## Supplementary Material

Refer to Web version on PubMed Central for supplementary material.

## Abbreviations

| | |
|---|---|
| **DMNQ** | 2,3-dimethoxy-1,4-naphthoquinone |
| **2-DG** | 2-deoxy-D-glucose |
| **ECAR** | extracellular acidification rate |
| **FCCP** | carbonyl cyanide 4-(trifluoromethoxy) phenylhydrazone |
| **HNE** | 4-hydroxynonenal |
| **OCR** | oxygen consumption rate |
| **RA** | retinoic acid |
| **ROS/RLS** | reactive oxygen species/reactive lipid species |

## Acknowledgments

## Reference List

1. Malkus KA, Tsika E, Ischiropoulos H. Oxidative modifications, mitochondrial dysfunction, and impaired protein degradation in Parkinson's disease: how neurons are lost in the Bermuda triangle. Mol. Neurodegener. 2009; 4:24. [PubMed: 19500376]

2. Choi SW, Gerencser AA, Nicholls DG. Bioenergetic analysis of isolated cerebrocortical nerve terminals on a microgram scale: spare respiratory capacity and stochastic mitochondrial failure. J. Neurochem. 2009; 109:1179–1191. [PubMed: 19519782]

3. Scott ID, Nicholls DG. Energy transduction in intact synaptosomes. Influence of plasma-membrane depolarization on the respiration and membrane potential of internal mitochondria determined in situ. Biochem. J. 1980; 186:21–33. [PubMed: 7370008]

4. Nicholls DG, Johnson-Cadwell L, Vesce S, Jekabsons M, Yadava N. Bioenergetics of mitochondria in cultured neurons and their role in glutamate excitotoxicity. J. Neurosci. Res. 2007; 85:3206–3212. [PubMed: 17455297]

5. Almeida A, gado-Esteban M, Bolanos JP, Medina JM. Oxygen and glucose deprivation induces mitochondrial dysfunction and oxidative stress in neurones but not in astrocytes in primary culture. J. Neurochem. 2002; 81:207–217. [PubMed: 12064468]

6. Dranka BP, Hill BG, Darley-Usmar VM. Mitochondrial reserve capacity in endothelial cells: The impact of nitric oxide and reactive oxygen species. Free Radic. Biol. Med. 2010; 48:905–914. [PubMed: 20093177]

7. Parker WD Jr, Parks JK, Swerdlow RH. Complex I deficiency in Parkinson's disease frontal cortex. Brain Res. 2008; 1189:215–218. [PubMed: 18061150]

8. Warburg OH. The classic: The chemical constitution of respiration ferment. Clin. Orthop. Relat Res. 2010; 468:2833–2839. [PubMed: 20809165]

9. Warburg O. On respiratory impairment in cancer cells. Science. 1956; 124:269–270. [PubMed: 13351639]

10. Warburg O. On the origin of cancer cells. Science. 1956; 123:309–314. [PubMed: 13298683]

11. Xie HR, Hu LS, Li GY. SH-SY5Y human neuroblastoma cell line: in vitro cell model of dopaminergic neurons in Parkinson's disease. Chin Med. J. (Engl.). 2010; 123:1086–1092. [PubMed: 20497720]

12. Agholme L, Lindstrom T, Kagedal K, Marcusson J, Hallbeck M. An In Vitro Model for Neuroscience: Differentiation of SH-SY5Y Cells into Cells with Morphological and Biochemical Characteristics of Mature Neurons. J. Alzheimers. Dis. 2010; 20:1069–1082. [PubMed: 20413890]

13. Lopes FM, Schroder R, da FM Jr, Zanotto-Filho A, Muller CB, Pires AS, Meurer RT, Colpo GD, Gelain DP, Kapczinski F, et al. Comparison between proliferative and neuron-like SH-SY5Y cells as an in vitro model for Parkinson disease studies. Brain Res. 2010; 1337:85–94. [PubMed: 20380819]

14. Luchtman DW, Song C. Why SH-SY5Y cells should be differentiated. Neurotoxicology. 2010; 31:164–165. [PubMed: 19895843]

15. Cheung YT, Lau WK, Yu MS, Lai CS, Yeung SC, So KF, Chang RC. Effects of all-trans-retinoic acid on human SH-SY5Y neuroblastoma as in vitro model in neurotoxicity research. Neurotoxicology. 2009; 30:127–135. [PubMed: 19056420]

16. Plowey ED, Cherra SJ III, Liu YJ, Chu CT. Role of autophagy in G2019S-LRRK2-associated neurite shortening in differentiated SH-SY5Y cells. J. Neurochem. 2008

17. Constantinescu R, Constantinescu AT, Reichmann H, Janetzky B. Neuronal differentiation and long-term culture of the human neuroblastoma line SH-SY5Y. J. Neural Transm. Suppl. 2007:17–28. [PubMed: 17982873]

18. Presgraves SP, Ahmed T, Borwege S, Joyce JN. Terminally differentiated SH-SY5Y cells provide a model system for studying neuroprotective effects of dopamine agonists. Neurotox. Res. 2004; 5:579–598. [PubMed: 15111235]

19. Biedler JL, Helson L, Spengler BA. Morphology and growth, tumorigenicity, and cytogenetics of human neuroblastoma cells in continuous culture. Cancer Res. 1973; 33:2643–2652. [PubMed: 4748425]

20. Sayre LM, Zelasko DA, Harris PL, Perry G, Salomon RG, Smith MA. 4-Hydroxynonenal-derived advanced lipid peroxidation end products are increased in Alzheimer's disease. J. Neurochem. 1997; 68:2092–2097. [PubMed: 9109537]

21. Yoritaka A, Hattori N, Uchida K, Tanaka M, Stadtman ER, Mizuno Y. Immunohistochemical detection of 4-hydroxynonenal protein adducts in Parkinson disease. Proc. Natl. Acad. Sci. U. S. A. 1996; 93:2696–2701. [PubMed: 8610103]

22. LoPachin RM, Gavin T, Petersen DR, Barber DS. Molecular mechanisms of 4-hydroxy-2-nonenal and acrolein toxicity: nucleophilic targets and adduct formation. Chem. Res. Toxicol. 2009; 22:1499–1508. [PubMed: 19610654]

23. Gueraud F, Atalay M, Bresgen N, Cipak A, Eckl PM, Huc L, Jouanin I, Siems W, Uchida K. Chemistry and biochemistry of lipid peroxidation products. Free Radic. Res. 2010; 44:1098–1124. [PubMed: 20836659]

24. Poli G, Schaur RJ, Siems WG, Leonarduzzi G. 4-hydroxynonenal: a membrane lipid oxidation product of medicinal interest. Med. Res. Rev. 2008; 28:569–631. [PubMed: 18058921]

25. Voss P, Siems W. Clinical oxidation parameters of aging. Free Radic. Res. 2006; 40:1339–1349. [PubMed: 17090423]

26. Siems W, Grune T, Sommerburg O, Flohe L, Cadenas E. HNE and Further Lipid Peroxidation Products. Biofactors. 2005; 24:1–4. [PubMed: 16403958]

27. Siems W, Grune T. Intracellular metabolism of 4-hydroxynonenal. Mol. Aspects Med. 2003; 24:167–175. [PubMed: 12892994]

28. Ullrich O, Henke W, Grune T, Siems WG. The effect of the lipid peroxidation product 4-hydroxynonenal and of its metabolite 4-hydroxynonenoic acid on respiration of rat kidney cortex mitochondria. Free Radic. Res. 1996; 24:421–427. [PubMed: 8804985]

29. Hill BG, Dranka BP, Zou L, Chatham JC, rley-Usmar VM. Importance of the bioenergetic reserve capacity in response to cardiomyocyte stress induced by 4-hydroxynonenal. Biochem. J. 2009; 424:99–107. [PubMed: 19740075]

30. Hill BG, Awe SO, Vladykovskaya E, Ahmed Y, Liu SQ, Bhatnagar A, Srivastava S. Myocardial ischaemia inhibits mitochondrial metabolism of 4-hydroxy-trans-2-nonenal. Biochem. J. 2009; 417:513–524. [PubMed: 18800966]

31. Picklo MJ, Amarnath V, McIntyre JO, Graham DG, Montine TJ. 4-Hydroxy-2(E)-nonenal inhibits CNS mitochondrial respiration at multiple sites. J. Neurochem. 1999; 72:1617–1624. [PubMed: 10098869]

32. Humphries KM, Yoo Y, Szweda LI. Inhibition of NADH-linked mitochondrial respiration by 4-hydroxy-2-nonenal. Biochemistry. 1998; 37:552–557. [PubMed: 9425076]

33. Liu W, Porter NA, Schneider C, Brash AR, Yin H. Formation of 4-hydroxynonenal from cardiolipin oxidation: Intramolecular peroxyl radical addition and decomposition. Free Radic. Biol. Med. 2011; 50:166–178. [PubMed: 21047551]

34. Watanabe N, Forman HJ. Autoxidation of extracellular hydroquinones is a causative event for the cytotoxicity of menadione and DMNQ in A549-S cells. Arch. Biochem. Biophys. 2003; 411:145–157. [PubMed: 12590933]

35. LaVoie MJ, Hastings TG. Dopamine quinone formation and protein modification associated with the striatal neurotoxicity of methamphetamine: evidence against a role for extracellular dopamine. J. Neurosci. 1999; 19:1484–1491. [PubMed: 9952424]

36. Mosmann T. Rapid colorimetric assay for cellular growth and survival: application to proliferation and cytotoxicity assays. J. Immunol. Methods. 1983; 65:55–63. [PubMed: 6606682]

37. Zhang J, Dong M, Li L, Fan Y, Pathre P, Dong J, Lou D, Wells JM, Olivares-Villagomez D, Van KL, et al. Endonuclease G is required for early embryogenesis and normal apoptosis in mice. Proc. Natl. Acad. Sci. U. S. A. 2003; 100:15782–15787. [PubMed: 14663139]

38. Gerencser AA, Neilson A, Choi SW, Edman U, Yadava N, Oh RJ, Ferrick DA, Nicholls DG, Brand MD. Quantitative microplate-based respirometry with correction for oxygen diffusion. Anal. Chem. 2009; 81:6868–6878. [PubMed: 19555051]

39. Ferrick DA, Neilson A, Beeson C. Advances in measuring cellular bioenergetics using extracellular flux. Drug Discov. Today. 2008; 13:268–274. [PubMed: 18342804]

40. Wu M, Neilson A, Swift AL, Moran R, Tamagnine J, Parslow D, Armistead S, Lemire K, Orrell J, Teich J, et al. Multiparameter metabolic analysis reveals a close link between attenuated mitochondrial bioenergetic function and enhanced glycolysis dependency in human tumor cells. Am. J. Physiol Cell Physiol. 2007; 292:C125–C136. [PubMed: 16971499]

41. Villani G, Attardi G. In vivo control of respiration by cytochrome c oxidase in human cells. Free Radic. Biol. Med. 2000; 29:202–210. [PubMed: 11035248]

42. Villani G, Greco M, Papa S, Attardi G. Low reserve of cytochrome c oxidase capacity in vivo in the respiratory chain of a variety of human cell types. J. Biol. Chem. 1998; 273:31829–31836. [PubMed: 9822650]

43. Brand MD, Nicholls DG. Assessing mitochondrial dysfunction in cells. Biochem. J. 2011; 437:575.

44. Brown GC, Lakin-Thomas PL, Brand MD. Control of respiration and oxidative phosphorylation in isolated rat liver cells. Eur. J. Biochem. 1990; 192:355–362. [PubMed: 2209591]

45. Brown GC. The leaks and slips of bioenergetic membranes. FASEB J. 1992; 6:2961–2965. [PubMed: 1644259]

46. Brand MD. The proton leak across the mitochondrial inner membrane. Biochim. Biophys. Acta. 1990; 1018:128–133. [PubMed: 2393654]

47. Sansbury BE, Riggs DW, Brainard RE, Salabei JK, Jones SP, Hill BG. Responses of hypertrophied myocytes to reactive species: implications for glycolysis and electrophile metabolism. Biochem. J. 2011

48. Biedler JL, Roffler-Tarlov S, Schachner M, Freedman LS. Multiple neurotransmitter synthesis by human neuroblastoma cell lines and clones. Cancer Res. 1978; 38:3751–3757. [PubMed: 29704]

49. Birket MJ, Orr AL, Gerencser AA, Madden DT, Vitelli C, Swistowski A, Brand MD, Zeng X. A reduction in ATP demand and mitochondrial activity with neural differentiation of human embryonic stem cells. J. Cell Sci. 2011; 124:348–358. [PubMed: 21242311]

50. Herrero-Mendez A, Almeida A, Fernandez E, Maestre C, Moncada S, Bolanos JP. The bioenergetic and antioxidant status of neurons is controlled by continuous degradation of a key glycolytic enzyme by APC/C-Cdh1. Nat. Cell Biol. 2009; 11:747–752. [PubMed: 19448625]

51. Sansbury BE, Jones SP, Riggs DW, rley-Usmar VM, Hill BG. Bioenergetic function in cardiovascular cells: The importance of the reserve capacity and its biological regulation. Chem. Biol. Interact. 2010

52. Yadava N, Nicholls DG. Spare respiratory capacity rather than oxidative stress regulates glutamate excitotoxicity after partial respiratory inhibition of mitochondrial complex I with rotenone. J. Neurosci. 2007; 27:7310–7317. [PubMed: 17611283]

53. Oliveira JM, Chen S, Almeida S, Riley R, Goncalves J, Oliveira CR, Hayden MR, Nicholls DG, Ellerby LM, Rego AC. Mitochondrial-dependent Ca2+ handling in Huntington's disease striatal cells: effect of histone deacetylase inhibitors. J. Neurosci. 2006; 26:11174–11186. [PubMed: 17065457]

54. Esteves AR, Domingues AF, Ferreira IL, Januario C, Swerdlow RH, Oliveira CR, Cardoso SM. Mitochondrial function in Parkinson's disease cybrids containing an nt2 neuron-like nuclear background. Mitochondrion. 2008; 8:219–228. [PubMed: 18495557]

55. Kiningham KK, Cardozo ZA, Cook C, Cole MP, Stewart JC, Tassone M, Coleman MC, Spitz DR. All-trans-retinoic acid induces manganese superoxide dismutase in human neuroblastoma through NF-kappaB. Free Radic. Biol. Med. 2008; 44:1610–1616. [PubMed: 18280257]

56. Landar A, Zmijewski JW, Dickinson DA, Le GC, Johnson MS, Milne GL, Zanoni G, Vidari G, Morrow JD, Darley-Usmar VM. Interaction of electrophilic lipid oxidation products with mitochondria in endothelial cells and formation of reactive oxygen species. Am. J. Physiol Heart Circ. Physiol. 2006; 290:H1777–H1787. [PubMed: 16387790]

57. Oliva CR, Nozell SE, Diers A, McClugage SG III, Sarkaria JN, Markert JM, rley-Usmar VM, Bailey SM, Gillespie GY, Landar A, et al. Acquisition of temozolomide chemoresistance in gliomas leads to remodeling of mitochondrial electron transport chain. J. Biol. Chem. 2010; 285:39759–39767. [PubMed: 20870728]
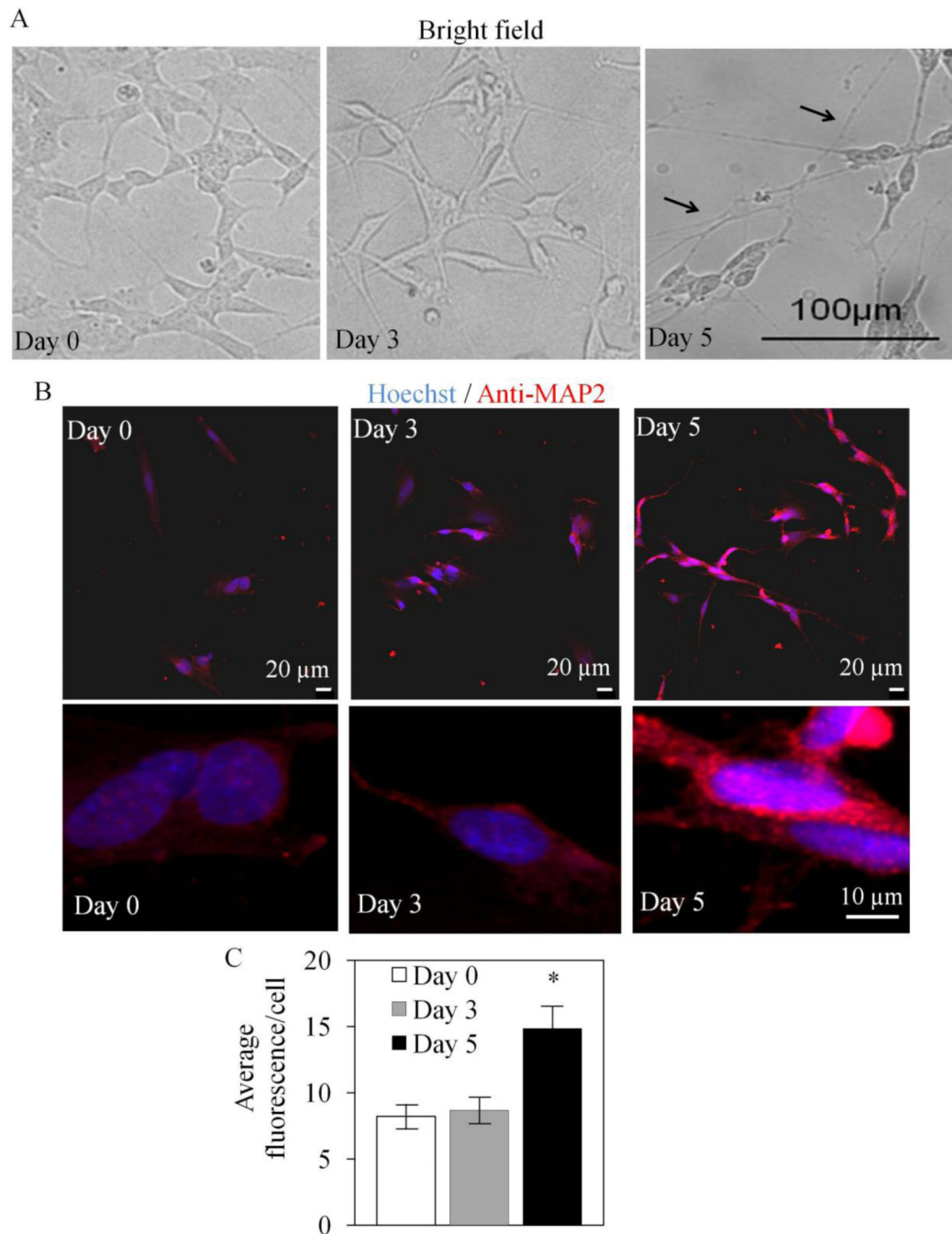
**Figure 1. Retinoic acid induced differentiation of SH-SY5Y cells**
(A) Bright field images of cells after retinoic acid treatment for 0, 3 and 5 days. Neurite extension was evident in Day 5 cells (arrows). (B) Low and high magnification images of nuclear stain by Hoechst and MAP2 immunostaining were captured by confocal microscopy with Day 0, Day 3 and Day 5 cells. Scale bar = 20 microns. (C) Quantitation of anti-MAP2 immunofluorescence intensity from panel B with Day 0, Day 3 and Day 5 cells. Quantification was performed with ≥ 84 cells for each of retinoic acid treatment days. Data = mean ± SEM. *$p$ <0.05 Student *t*-test compared to Day 0.
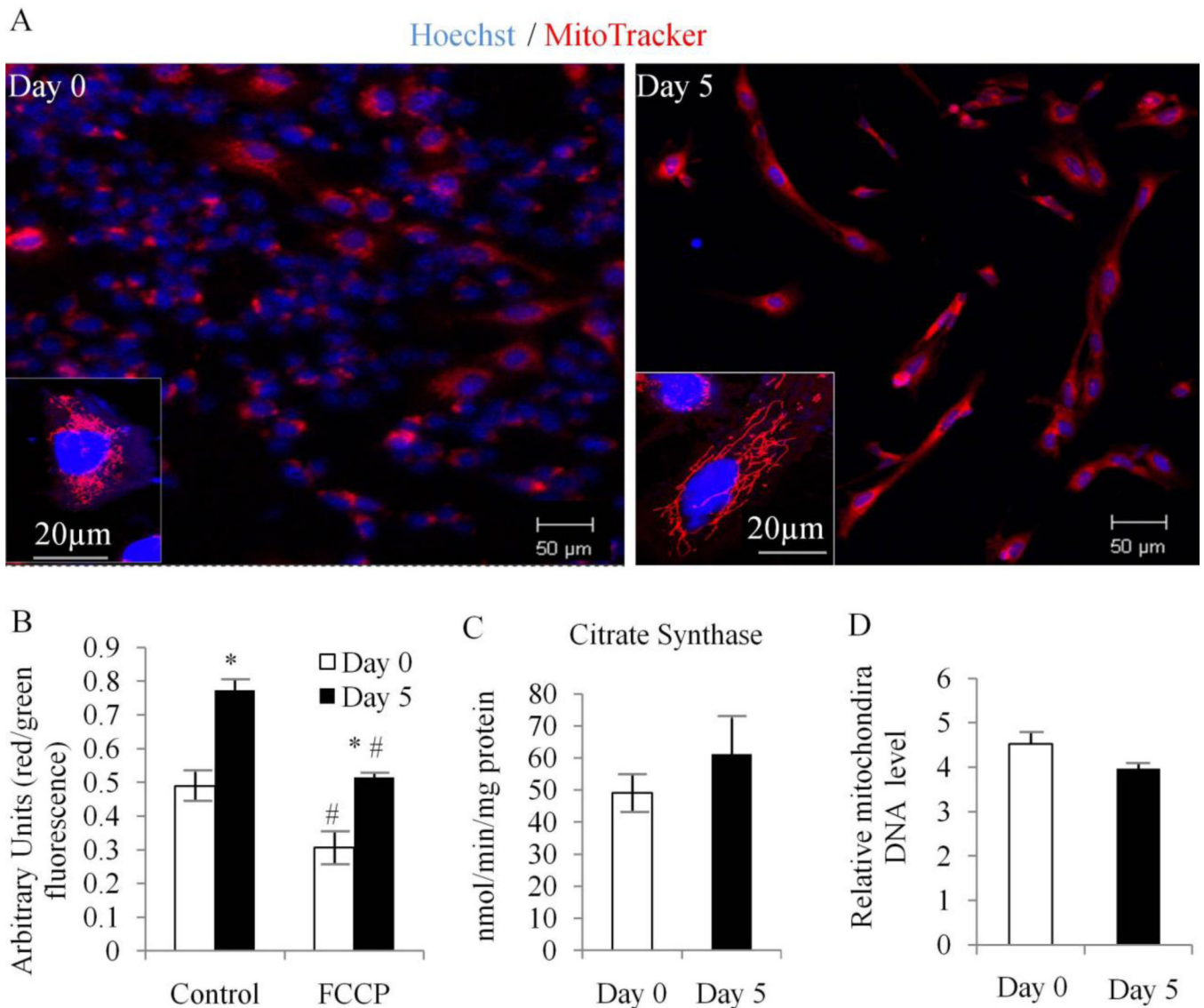
**Figure 2. Differentiated SH-SY5Y cells exhibit increased mitochondrial network and higher membrane potential without changing mitochondrial mass**

(A) SH-SY5Y cells were treated with retinoic acid for 0, 3, and 5 days. MitoTracker Red was loaded to the cells. Low (taken at $10 \times$ lens and compiled by montage) and high magnification images (taken at $100 \times$ lens) were captured by confocal microscopy. (B) Mitochondrial membrane potential assessments with JC-1 staining. Day 5 cells have higher baseline membrane potential (Control) as assessed by JC-1. 10 µM FCCP decreased membrane potentials in both Day 0 and Day 5 cells. *$p$ <0.05 Student $t$-test compared to Day 0. # $p$ <0.05 Student $t$-test compared to Control. (D) Citrate synthase activities are comparable between Day 0 and Day 5 SH-SY5Y cell extracts. Cells were lysed in phosphate buffer containing 3% (w/v) lauryl maltoside. Each assay contained 5 – 50 µg of cell lysate. Data was normalized to total protein. n=4. (E) Mitochondrial DNA copy number per cell is comparable between Day 0 and Day 5 SH-SY5Y. DNA was isolated from SH-SY5Y cells. Mitochondrial and nuclear 18S DNA copy numbers were quantitated with real-time PCR. Mitochondrial DNA was normalized to 18S nuclear DNA. n=3.
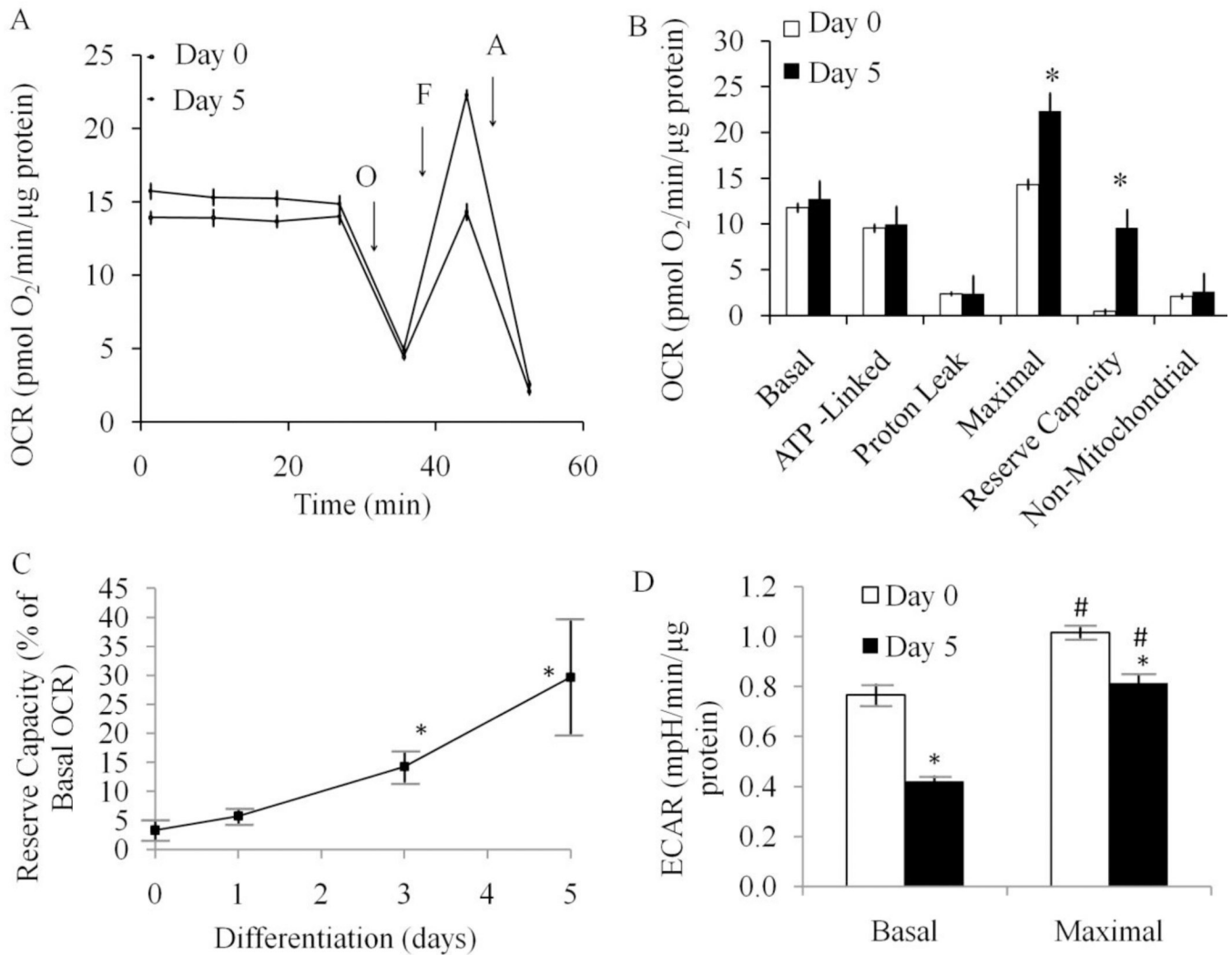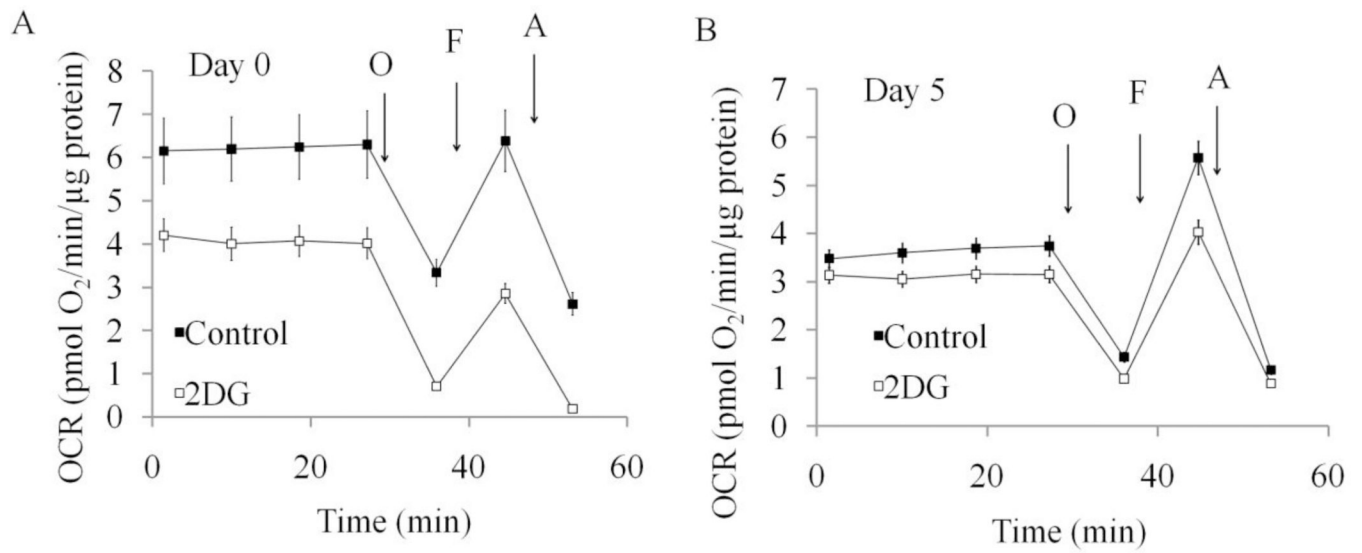
**Figure 3. Differentiated SH-SY5Y cells exhibit increased mitochondrial reserve capacity compared to undifferentiated SH-SY5Y cells**

Cells were seeded into specialized 24-well Seahorse Biosciences V7 microplates then bioenergetic function was assessed using the Seahorse XF24 Analyzer. Both oxygen consumption rate (OCR) and extracellular acidification rate (ECAR) were measured. ATP synthase inhibitor oligomycin (**O**, 1 µM), uncoupler FCCP (**F,** 1 µM) and complex III inhibitor antimycin A (**A,** 10 µM) were injected at indicated times to determine different parameters of mitochondrial functions. (A) OCR as pmol $O_2$/min/µg protein, n=5 for each experiment. Data = mean ± SEM. (B) Bar graph comparison of basal, ATP-linked, proton leak-linked, maximal, non-mitochondrial oxygen consumption of Day 0 and Day 5 cells. Non-mitochondrial OCR was determined as the OCR after antimycin A treatment. Basal OCR was determined as OCR before oligomycin minus OCR after antimycin A. ATP-lined OCR was determined as OCR before oligomycin minus OCR after oligomycin. Proton leak was determined as Basal OCR minus ATP-linked OCR. Maximal was determined as the OCR after FCCP minus non-mitochondrial OCR. Reserve Capacity was defined as the difference between Maximal OCR after FCCP minus Basal OCR. Statistical analyses were carried out by Student *t*-test. \**p* <0.05 compared between Day 0 and Day 5 samples. Data = mean ± SEM. (C) Reserve Capacity is plotted as a percentage of basal OCR against differentiation days after 0, 1, 3, and 5 days of retinoic acid treatment. n=5 for each

experiments. Statistical analyses were carried out by Student t-test. *$p$ <0.05 compared to Day 0. Data = mean ± SEM. (D) Extracellular acidification rate (ECAR) was plotted for Day 0 and Day 5 cells. Basal ECAR was plotted at the time before oligomycin injection (open bars). Maximal ECAR was plotted after oligomycin injection (closed bars). Data = mean ± SEM. Statistical analyses were carried out by Student t-test. *$p$ <0.05 compared to Day 0. # $p$ <0.05 compared to Basal.

**Figure 4. Inhibition of glycolysis by 2-DG changes reserve capacity in differentiated cells**
(A) OCR of Day 0 undifferentiated SH-SY5Y cells without and with 2-DG treatment for 24 hours. (B) OCR of Day 5 differentiated SH-SY5Y cells without and with 2-DG treatment for 24 hours. ATP synthase inhibitor oligomycin (**O**), uncoupler FCCP (**F**) and complex III inhibitor antimycin A (**A**) were injected at indicated times to determine different parameters of mitochondrial functions. Data = mean ± SEM.
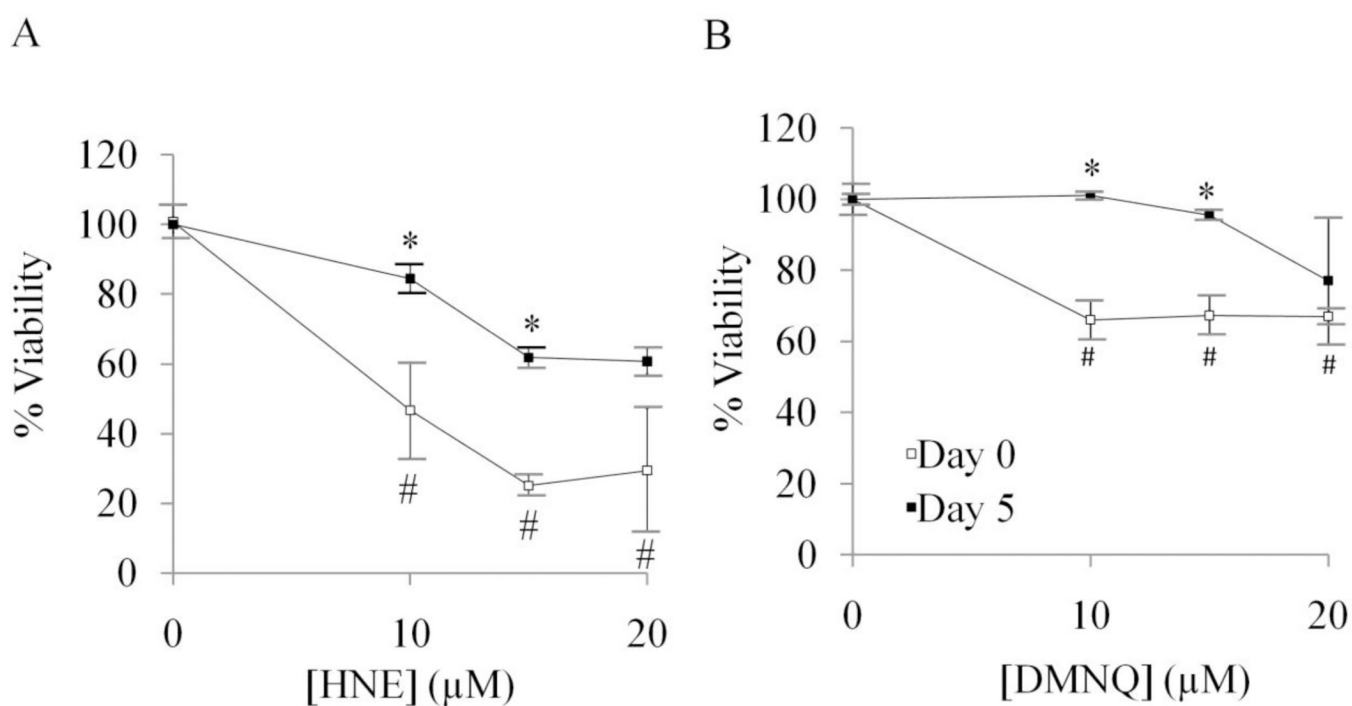
**Figure 5. Differentiated SH-SY5Y cells are more resistant to HNE or DMNQ-induced cell death**
(A) Cell viability of undifferentiated (Day 0) and differentiated (Day 5) SH-SY5Y cells after treatment with 0–20 µM HNE, determined by MTT assay. (B) Cell viability of undifferentiated (Day 0) and differentiated (Day 5) SH-SY5Y cells after treatment with 0–20 µM DMNQ, determined by MTT assay. Data = mean ± SEM. *$p$ <0.05 Student $t$-test compared to Day 0. # $p$<0.05 compared to 0 µM treatment.
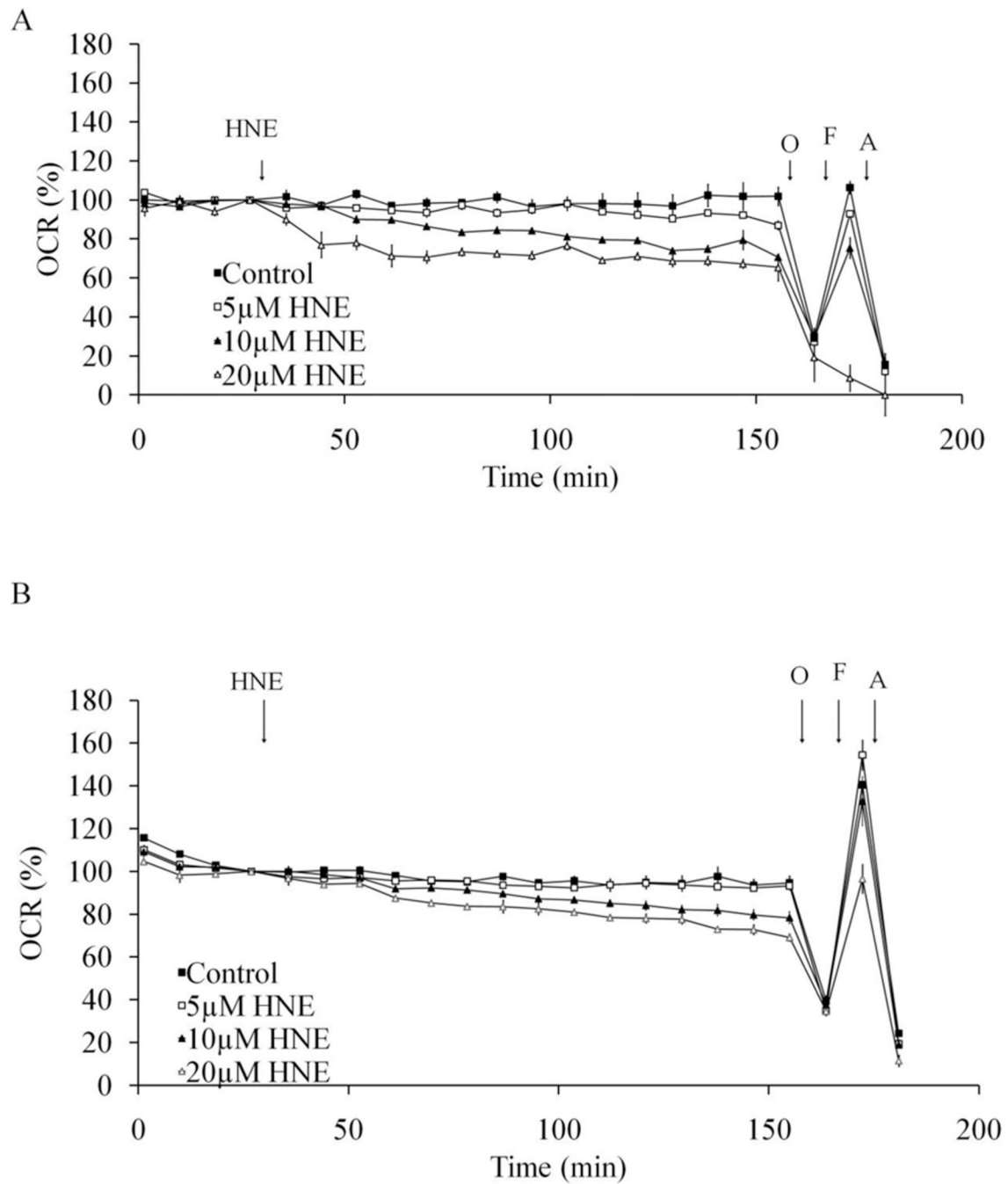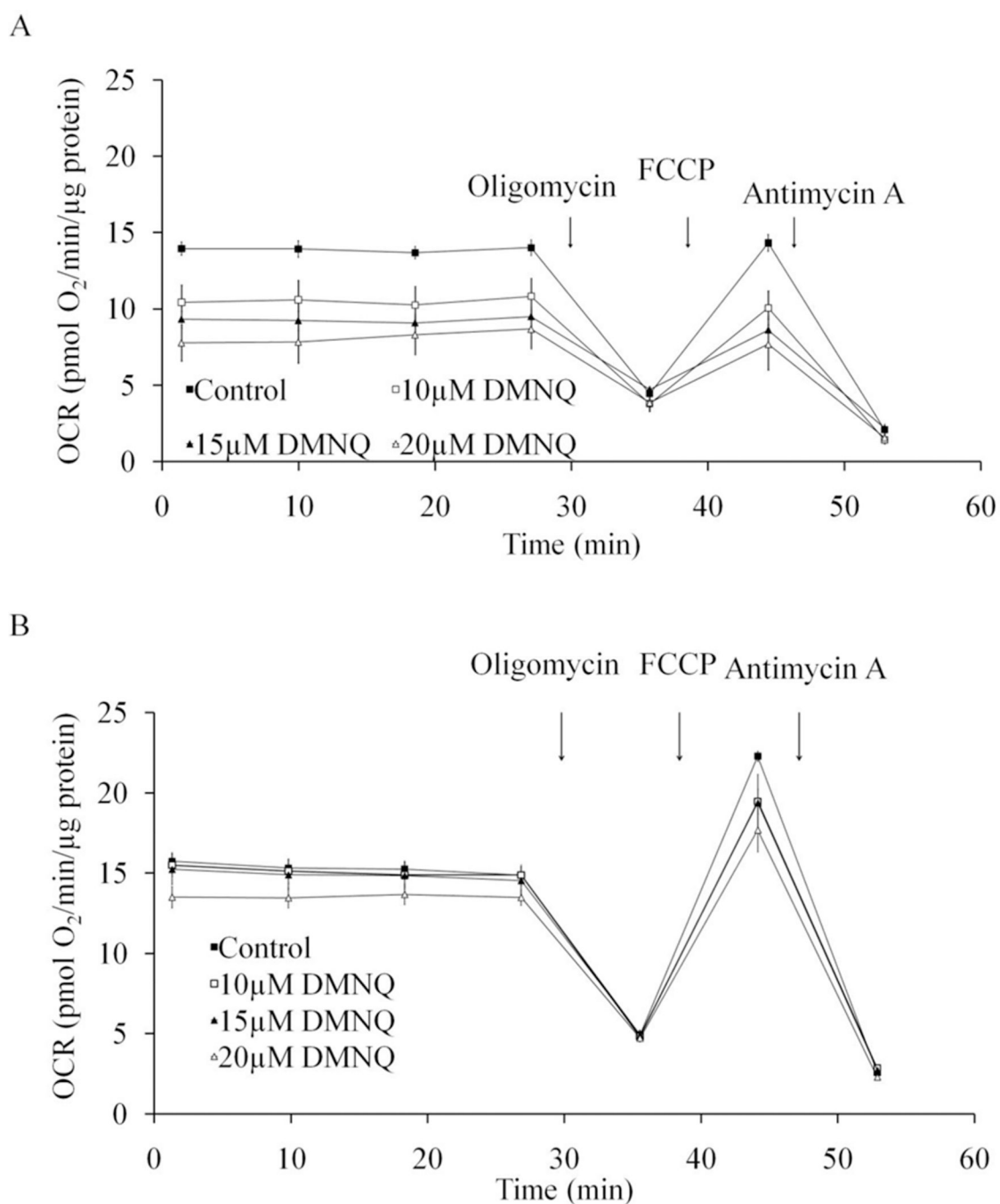
**Figure 6. Resilience of mitochondrial function in response to HNE in differentiated SH-SY5Y cells compared to undifferentiated cells**

(A) OCR of Day 0 undifferentiated SH-SY5Y cells treated with 0–20 µM HNE. Basal OCR levels ranged from 122–177 pmol $O_2$/min. (B) OCR of Day 5 differentiated SH-SY5Y cells treated with 0–20 µM HNE. Basal OCR ranged from 230–559 pmol $O_2$/min. HNE was injected at 30 min of OCR measurement and continued for 2 hr, followed by injection of oligomycin (**O**), FCCP (**F**) and antimycin A (**A**) at indicated times. Data = mean ± SEM.
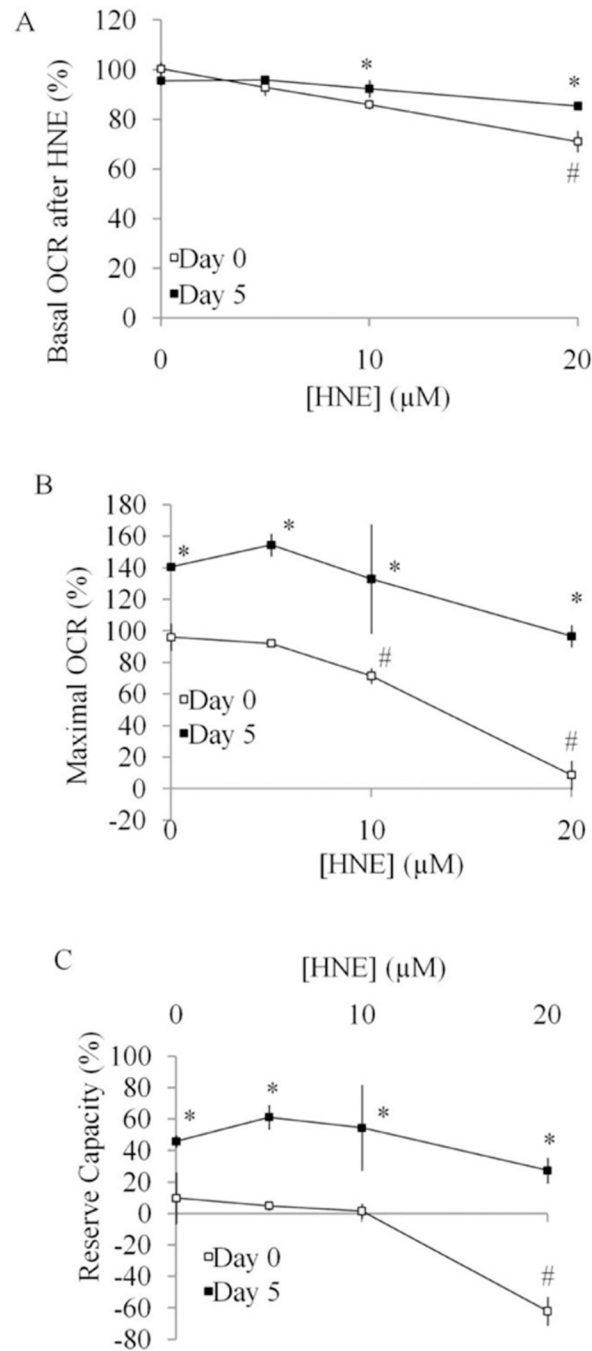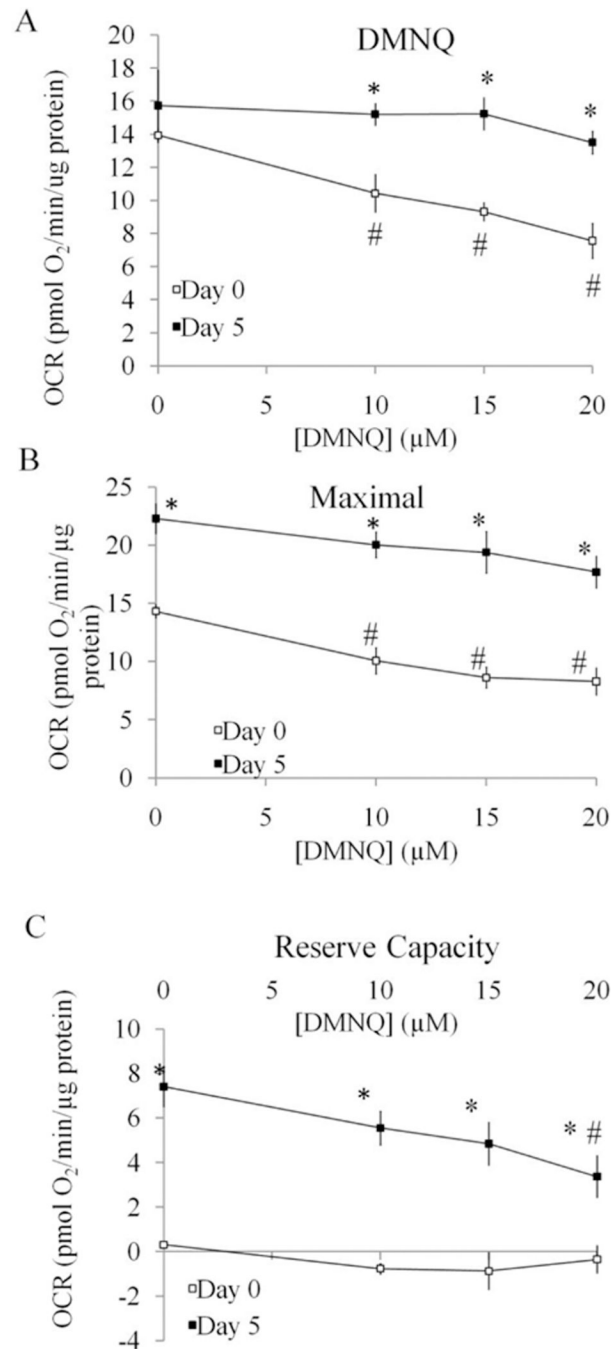
**Figure 7. Comparison of parameters of mitochondrial function between Day 0 undifferentiated SH-SY5Y cells and Day 5 differentiated cells in response to HNE treatment**
(A) Basal OCR after HNE (determined as OCR at 50 min after HNE injection normalized against the OCR before HNE injection) was plotted with increasing doses of treatment with HNE. (B) Maximal OCR (determined as OCR after FCCP injection normalized against OCR before oligomycin injection) was plotted with increasing doses of treatment with HNE. (C) Reserve capacity (determined as OCR after FCCP injection minus OCR before oligomycin injection followed by normalization against OCR before oligomycin injection) was plotted with increasing doses of treatment with HNE. Data = mean ± SEM. *$p < 0.05$ Student *t*-test compared to Day 0. # $p < 0.05$ compared to 0 µM treatment.

**Figure 8. Resilience of mitochondrial function in response to DMNQ in differentiated SH-SY5Y cells compared to undifferentiated cells**
DMNQ was added to cells for 4 hr before OCR measurement and continued for 30 min, followed by injection of oligomycin (**O**), FCCP (**F**) and antimycin A (**A**) at indicated times. (A) OCR of Day 0 undifferentiated SH-SY5Y cells treated with 0–20 μM DMNQ. (B) OCR of Day 5 differentiated SH-SY5Y cells treated with 0–20 μM DMNQ. Data = mean ± SEM. OCR was normalized to protein.

**Figure 9. Comparison of parameters of mitochondrial function between Day 0 undifferentiated SH-SY5Y cells and Day 5 differentiated cells in response to DMNQ treatment**
(A) DMNQ OCR (determined as OCR before oligomycin injection) was plotted with increasing doses of treatment with DMNQ. (B) Maximal OCR (determined as OCR after FCCP injection minus OCR after antimycin injection) was plotted with increasing doses of treatment with DMNQ. (C) Reserve capacity (determined as OCR after FCCP injection minus OCR before oligomycin injection) was plotted with increasing doses of treatment with DMNQ. Data = mean ± SEM. *$p$ <0.05 Student $t$-test compared to Day 0. # $p$ <0.05 compared to 0 µM treatment.
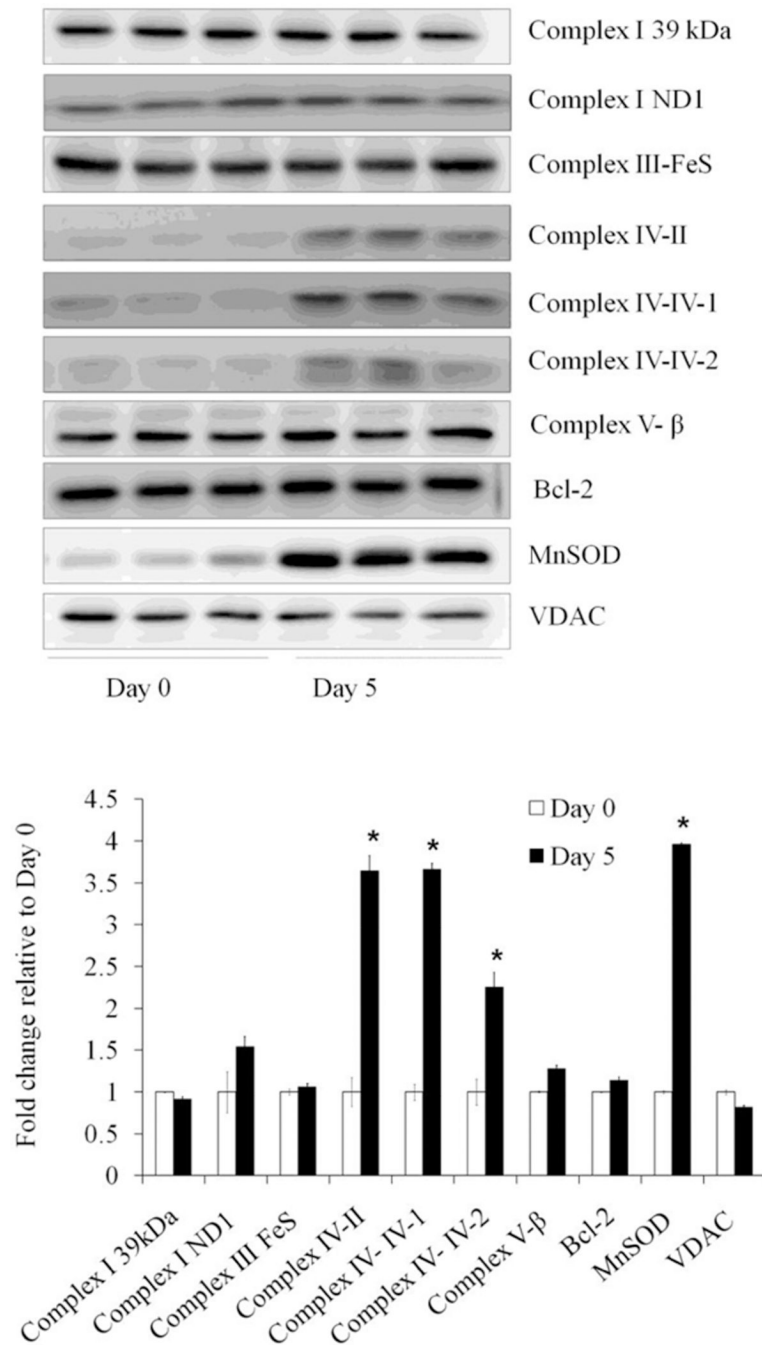
**Figure 10. Mitochondrial protein levels in differentiated and undifferentiated SH-SY5Y cells**
Western blot analyses of mitochondrial inner membrane protein Complex I-subunit 39 kDa, Complex I-subunit ND1, Complex III-FeS, Complex IV-subunit II, Complex IV-subunit IV-isoform 1, Complex IV-subunit IV-isoform 2, Complex V-β subunit, outer membrane protein VDAC, matrix protein MnSOD, Cytochrome C, and Bcl-2Ponceus S staining intensity of the whole gel was used for loading control. Data = mean ± SEM. n=3–10. Bar graph shows the quantification. * $p$ <0.05 by Student $t$-test compared between Day 0 and Day 5.